Journal of Hydrology 550 (2017) 230–238

Contents lists available at ScienceDirect

Journal of Hydrology

journal homepage: www.elsevier.com/locate/jhydrol

Research papers

Estimation of the spatiotemporal dynamics of snow covered area by using cellular automata models

Eulogio Pardo-Igúzquiza [a], Antonio-Juan Collados-Lara [b,*], David Pulido-Velazquez [b,c]

[a] Instituto Geológico y Minero de España (IGME), Ríos Rosas, 23, 28003 Madrid, Spain
[b] Instituto Geológico y Minero de España (IGME), Urb. Alcázar del Genil, 4, bajo, Edificio Zulema, 18006 Granada, Spain
[c] Departamento de Ciencias Politécnicas, Escuela Universitaria Politécnica, Universidad Católica San Antonio de Murcia (UCAM), Murcia, Spain

ARTICLE INFO

Article history:
Received 12 November 2016
Received in revised form 18 April 2017
Accepted 26 April 2017
Available online 5 May 2017
This manuscript was handled by Corrado Corradini, Editor-in-Chief, with the assistance of Masaki Hayashi, Associate Editor

Keywords:
Snowline
Cellular automata
Elevation
Climatological indexes
Sierra Nevada

ABSTRACT

Given the need to consider the cryosphere in water resources management for mountainous regions, the purpose of this paper is to model the daily spatially distributed dynamics of snow covered area (SCA) by using calibrated cellular automata models. For the operational use of the calibrated model, the only data requirements are the altitude of each cell of the spatial discretization of the area of interest and precipitation and temperature indexes for the area of interest. For the calibration step, experimental snow covered area data are needed. Potential uses of the model are to estimate the snow covered area when satellite data are absent, or when they provide a temporal resolution different from the operational resolution, or when the satellite images are useless because they are covered by clouds or because there has been a sensor failure. Another interesting application is the simulation of SCA dynamics for the snow covered area under future climatic scenarios. The model is applied to the Sierra Nevada mountain range, in southern Spain, which is home to significant biodiversity, contains important water resources in its snowpack, and contains the most meridional ski resort in Europe.

1. Introduction

Water resources management and operational river forecasts in river basins that enclose high mountainous regions must take into account the cryosphere (i.e. the snowpack). The amount of snow and its spatial and temporal distribution as well as the outflow of water from the snowpack must be estimated from available information. The problem is three-fold: (i) estimation of the snow covered area (SCA); (ii) estimation of the snowpack thickness and (iii) estimation of the snow density. The three variables (covered area, thickness and density) are needed to estimate the snow water equivalent, however estimating each variable is a problem in and of itself. Each variable can be approached by applying different modelling techniques: interpolation methods (e.g. Richer et al., 2013; Mir et al., 2015 to estimate SCA; Collados-Lara et al., 2017 to estimate snow pack thickness; Bormann et al., 2013 and Lopez-Moreno et al., 2013 to estimate snow density; Sexstone and Fassnacht, 2014 and Elder et al., 1998 to estimate snow water equivalent), conceptual methods (e.g. HBV (Lindström et al., 1997); Snowmelt Runoff Model (SRM) (Martinec et al., 2008; Sensoy and Uysal, 2012) or physically-based models (e.g. CROCUS (Bruland et al., 2001); ECHAM (Foster et al., 1996)). Under standard circumstances, SCA can be estimated using satellite data, such as from the Moderate Resolution Imaging Spectroradiometer (MODIS) (Hall et al., 2006; Hall and Riggs, 2007). The question we aim to answer in this work is how to estimate the snow covered area when satellite data are unavailable. Satellite data may be unavailable for different reasons. For instance it could be because the satellite was not launched yet or because the temporal resolution of the satellite data is larger than the temporal resolution of interest. Also satellite data may be useless because the area of interest was covered by clouds or because there was a failure in the sensor. Furthermore, future scenarios of precipitation and temperature could be defined from the simulation performed with different Regional Climatic Models (RCM) for the emission scenarios defined by IPCC (Jacob et al., 2013). These future scenarios of climate in an area, defined by applying a downscaling technique from the RCM simulations, could be used to feed the SCA model in order to assess future SCA scenarios. This is a method commonly applied to assess future scenarios of other hydrological variables from hydrological balance models (Pulido-Velazquez et al., 2011; Pulido-Velázquez et al., 2015). These hydrological model predictions could also be

* Corresponding author.
E-mail addresses: e.pardo@igme.es (E. Pardo-Igúzquiza), ajcollados@gmail.com (A.-J. Collados-Lara), d.pulido@igme.es (D. Pulido-Velazquez).

http://dx.doi.org/10.1016/j.jhydrol.2017.04.058
0022-1694/

improved by incorporating SCA using the data assimilation technique (Thirel et al., 2013; Alvarado Montero et al., 2016).

In addition to the physically-based or conceptual approaches (Molotch et al., 2004), we can also find examples of regression techniques (Richer et al., 2013; Mir et al., 2015) and learning algorithms (artificial neural networks) to estimate Snow Cover Fraction Mapping (Hou and Huang, 2014; Mishra et al., 2014). In this study we propose a novel approach to the problem: the application of an evolutionary algorithm, as the cellular automaton, to estimate SCA. The estimation of SCA fits perfectly in the kind of problems that can be analysed with cellular automata techniques, as they are complex, dynamic systems that can be approached in a discrete way. Cellular automata models are good for simulating complex discrete dynamics by using simple rules that define the interaction between neighbour cells that discretize the study area. They have been applied to different problems in geosciences like urban growth dynamics (Kumar et al., 2014), snow crystal growth (Reiter, 2005) or simulation of snow avalanches (Barpi et al., 2007), among others. Cellular automata have also been used to simulate snow cover dynamics (Leguizamón, 2006). However the latter reference offers only a preliminary study that had significant limitations: (i) it only uses a small synthetic area rather than a real study area, (ii) it simulates a simple dynamic situation of reduction of the snowpack from a starting condition with an existing snowpack, (iii) the simulation is for a short time interval, (iv) the simulation does not introduce driving climatological indexes (precipitation and temperature) in order to guide the dynamics, (v) the procedure cannot start a snowpack in an image where all the cells are without snow. In this paper we extend the idea of using cellular automata to estimate the snow covered area. The extension deals with overcoming each of the aforementioned limitations. We used a real case study so that the cellular automata could be calibrated and validated but the methodology is completely general and can be applied to any area of interest because the data requirements are minimal. The methodology is described in the next section.

2. Methodology

Cellular automata are discrete dynamic models introduced by Wolfram (1984) in order to simulate complex dynamics using simple rules of interaction. The two-dimensional area of interest (i.e. a geographical region projected on a plane) is divided into a finite number of cells or pixels. Time is also discretized in time steps. The shape and size of the study area can be arbitrary, but for the sake of presentation one can think of a rectangular grid of cells: $\{(i,j); i = 1,\ldots,N_x; j = 1,\ldots,N_y\}$. The size of the cell can be any of interest; for example in the case study we will use square cells measuring approximately 460 m × 460 m, which is the spatial resolution of a MODIS image for the latitude of the study area. As was already mentioned, there is also a discretization of time; for example in the case study the time step is one day. Next, each cell (i,j) can be, at each time, t, in one of two possible states (1 or 0):

$$S(i,j,t) = \begin{cases} 1 & \text{if cell}(i,j)\text{is covered by snow at time } t \\ 0 & \text{ifcell}(i,j)\text{is free of snow at time } t \end{cases} \quad (1)$$

The state $S(i,j,t)$ depends, in general, on:

- The state of the cell (i,j) at the previous time step: $S(i,j,t-1)$.
- The states, at the previous time step, of the cells of a given configuration of neighbour cells. For example for an 8-neighbourhood, the states of the cells $(i-1,j-1)$, $(i,j-1)$, $(i+1,j-1)$, $(i+1,j)$, $(i+1,j+1)$, $(i,j+1)$, $(i-1,j+1)$ and $(i-1,j)$ at time $t-1$ are involved.
- A given set of transition rules. In classic cellular automaton models, the transition rules depend on the state of the cell at the previous step and the states of the neighbour cells at the previous step. However, in order to simulate realistic snow dynamics, we must introduce transition rules defined by some driving variables. This can be defined as a mixed cellular automaton. We have chosen a couple climatological indexes as driving variables: precipitation and temperature, $P(t)$ and $T(t)$, respectively, and a terrain variable: the altitude $H(i,j)$ of each cell (i,j). This allows the cellular automaton to evolve even if all the cells of the study area are at state zero. The altitude index in the calculation cells has been obtained as the mean altitude from a digital elevation model which has a spatial resolution of 5 meters (the highest DEM resolution available from the National Geographic Institute of Spain). Temperature and precipitation indices are used in the form of two time series: a time series of daily temperature and a time series of daily precipitation. These time series could be measured at a weather station or obtained from a given estimation product. The absolute values of these indices are not important in this problem because they are calibrated for a specific problem. The truly important feature of these indices is that they capture the temporal climatological variability of the case study.

The cellular automata model is calibrated with experimental snow covered area data for a particular period of time. For example, in our case study the experimental data are daily binary images of snow/no snow cells obtained from MODIS images (Hall et al., 2006) and the calibration period lasts three years. Furthermore, in our case study (next section), the estimation time starts on 1 July of the first year of the calibration period when the state of every cell in the study area is equal to zero (there is no snow in the study area). Hence, a pure cellular automaton cannot work because all the cells have the same state of zero, or equivalently the snowline is at an arbitrarily high altitude, which is larger than the largest altitude in the study area. Thus by introducing the driving variables, the discrete system can follow the realistic dynamics of the snowpack by changing the snowline, which is defined as the altitude above which the terrain can have snow. Thus new transition rules are introduced by using the climatological indexes and the digital elevation model is:

- If the precipitation is larger than or equal to a given threshold, $P(t) \geqslant P_0$, and the altitude of the cell (i,j) is above the snowline $H(i,j) > H_k(t)$, the state of the cell will be 1 (that is, by remaining at state 1 if it was already 1 or by changing from state 0 to state 1). The snow line H_k is defined, discretized in K values, by the temperature index $T(t)$:

  If $T(t) < T_1$ then $H_k(t) = H_1$
  If $T(t) < T_2$ then $H_k(t) = H_2$
  ...
  If $T(t) < T_K$ then $H_k(t) = H_K$
  With $T_1 > T_2 > \ldots > T_K$ and $H_1 > H_2 > \ldots > H_K$.

- If precipitation at day t is below the threshold $P(t) < P_0$ and the temperature has decreased or has increased by an amount smaller than a given threshold:

$$T(t) - T(t-1) \leqslant T_c > 0 \quad (2)$$

then the state of each cell remains at the state of the previous time step.

- Otherwise, if precipitation at day t is below the threshold $P(t) < P_0$ and the temperature has increased by an amount larger than a given threshold

$$T(t) - T(t-1) > T_c > 0 \tag{3}$$

the state of a pixel in state 0 remains at state 0, and a pixel at state 1 changes to state 0 (fusion of snow) if the number of neighbour cells $N(i,j)$ with state 1 is smaller than a given threshold N_m:

$$N(i,j) \leqslant N_m \tag{4}$$

Thus $P_0, K, T_1, T_2, \ldots, T_K, H_1, H_2, \ldots, H_K, T_c, N_m$ are parameters to calibrate.

When representing the discretized snowline defined by the data pairs $(T_1, H_1; T_2, H_2; \ldots; T_K, H_K)$ they result in a straight line, thus the calibration can be simplified from $2K$ parameters to just two parameters, the slope b and the intercept a of the straight line:

$$H(t) = a + bT(t) \tag{5}$$

Thus the parameters to calibrate are P_0, a, b, T_c, N_m, which is a more amenable number of parameters. They are assigned optimal values using an optimization approach (search using the uniform mesh method) in which values are given to the parameters. The set of values which result in a minimum value for the mean squared error between experimental data and simulated snowpack for the calibration period are chosen as the parameters for the model.

3. Case study

Our case study is located in the Sierra Nevada mountain range, a Mediterranean high altitude mountain range in southern Spain (Fig. 1A). The area of interest is the domain in which we find the main snow pack of the Sierra Nevada mountain range. Nevertheless, for simplicity, the domain employed to simulate the SCA evolution was defined by using a rectangular portion of the MODIS mesh that includes the aforementioned area of interest. The final adopted mesh covers an area significantly wider than the main snowpack in the Sierra Nevada. Outside of this area within the mesh we can occasionally find some snow but it disappears in a few days. Fig. 1A shows the area of interest, where the probability of having snow is higher than six days every snow season. It has been obtained by using historical MODIS satellite data.

The domain dimensions are around 80 km in length (E-W direction) and between 15 and 30 km wide (N-S direction), giving a surface area of approximately 2000 km^2. The Sierra Nevada is a national park with significant biodiversity and it is home to the most meridional ski resort in Europe. The Sierra Nevada is also an important source of water resources, mainly from the accumulation of snow during the winter. The aim of this study is to estimate the daily dynamics of the snow covered area on a grid with square cells approximately 460 m long on each side, which correspond to the pixels of the MODIS image that covers the region. NASA has been collecting SCA information since 1966 at various temporal resolutions (1 day, 8 days and 1 month) and with an approximate spatial resolution of 463 m since 2000, using MODIS (Hall et al., 2006).

The daily SCA from MODIS provides the fractional covered area (in% for example). Because the automaton provides binary results for each pixel (snow or non-snow), in order to facilitate the comparison of snow spatial distribution with the satellite observation maps, we decided to use a binary satellite product to calibrate and validate the model. Nevertheless, instead of directly using the binary MODIS product (Hall et al., 2006) we used the fractional snow cover product in order to define our own binary product. We did this because we wanted to complete the snow information for pixels with cloudy conditions to define the satellite maps. We employed an interpolation method to estimate those "cloudy pixels" that can be only applied with the fractional snow covered area product before translating it into our binary product.

For cloudy days, the fractional snow cover in a pixel covered by clouds was estimated using a linear interpolation between the closest prior and next cloudless days. In our case, this provided a close enough approximation, taking into account that, in the historical period, the number of consecutive cloudy days in a pixel was quite small (the mean length of consecutive cloudy dates in a pixel is 2.2 days in the calibration period and 1.6 in the validation period) and the inertia of the snowpack in this alpine region is sufficient.

Finally, we transformed the completed fractional SCA product to a daily binary SCA image by using the unbiased transformation:

$$B(i,j,t) = \begin{cases} 1 & \text{if } F(i,j,t) \geqslant 50\% \\ 0 & \text{if } F(i,j,t) < 50\% \end{cases} \tag{6}$$

where $F(i,j,t)$ is the fractional SCA (in %) of the cell (i,j) at day t and $B(i,j,t)$ is the binary SCA of the cell (i,j) at day t. Thus the daily dynamics of SCA, that is the area covered by the snowpack, can be represented as a time series of the number of cells of SCA versus time.

In this study, a three year time span, from 1 July 2000 to 30 June 2003, was used for calibration purposes and another three year time span, from the 1 July 2003 to 30 June 2006, was used for validation purposes. As an example of the snow area dynamics for a given year, Fig. 2 shows the daily dynamics of the SCA for three consecutive years, from 1 July 2000 to 30 June 2003. From Fig. 2, it can be seen how the time series starts in the summer when there is no snow pack. The SCA is represented as number of cells where each cell has a surface area of 460 m × 460 m or 0.2116 km^2. For this particular time period, it can be seen how the dynamics may be very different from year to year with a different number of maxima each year. At the beginning of the snow season the SCA peaks are asymmetrical with rapid growth and a slower decrease but in the middle of the snow season the peaks are more symmetrical and show quick dynamics. The driving variables of precipitation and temperature can be calculated from many different sources, such as from the dataset SPAIN02 (Herrera et al., 2012, 2016). The Spain02 dataset is a daily temperature and precipitation estimation from the observational data (around 2500 quality-controlled stations) collected by the Spanish Meteorological Agency in the period 1971–2010. An assessment of the validation of some Spanish datasets, including Spain02, was recently carried out by Quintana-Seguí et al. (2016). We have employed version 4 (v4) of the SPAIN02 project dataset (http://www.meteo.unican.es/en/datasets/spain02), which includes daily field estimations with a spatial resolution of 0.11° in rotated coordinates matching Euro-CORDEX grids. The SPAIN02 dataset has already been employed in many research studies (Escriva-Bou et al., 2017; Fernandez-Montes and Rodrigo, 2015).

Even for this single dataset, different indices can be calculated, for example by using the mean precipitation of stations that have a certain altitude (a.s.l.). The altitude thresholds of 1000, 1500, 2000, 2500 and 3000 m (a.s.l.) have been used. For temperature, there are even more possibilities, as the minimum, mean or maximum temperature could be used. Also, with regard to precipitation, the mean temperatures above 1000, 1500, 2000, 2500 and 3000 m (a.s.l.) have been considered. Fig. 3 shows, for one year and for illustrative purposes, the daily temperature index calculated as the mean of the minimum temperatures above 1000 and 3000 m (Fig. 3A) and the mean of the maximum temperatures above 1000 and 3000 m (Fig. 3B). After trying the different combinations of precipitation indices (5 possibilities) and temperature indices (15 possibilities) the combination of precipitation above 1000 m and maximum temperature above 1000 m have been shown to be the best choice as climatological indices for the study area.

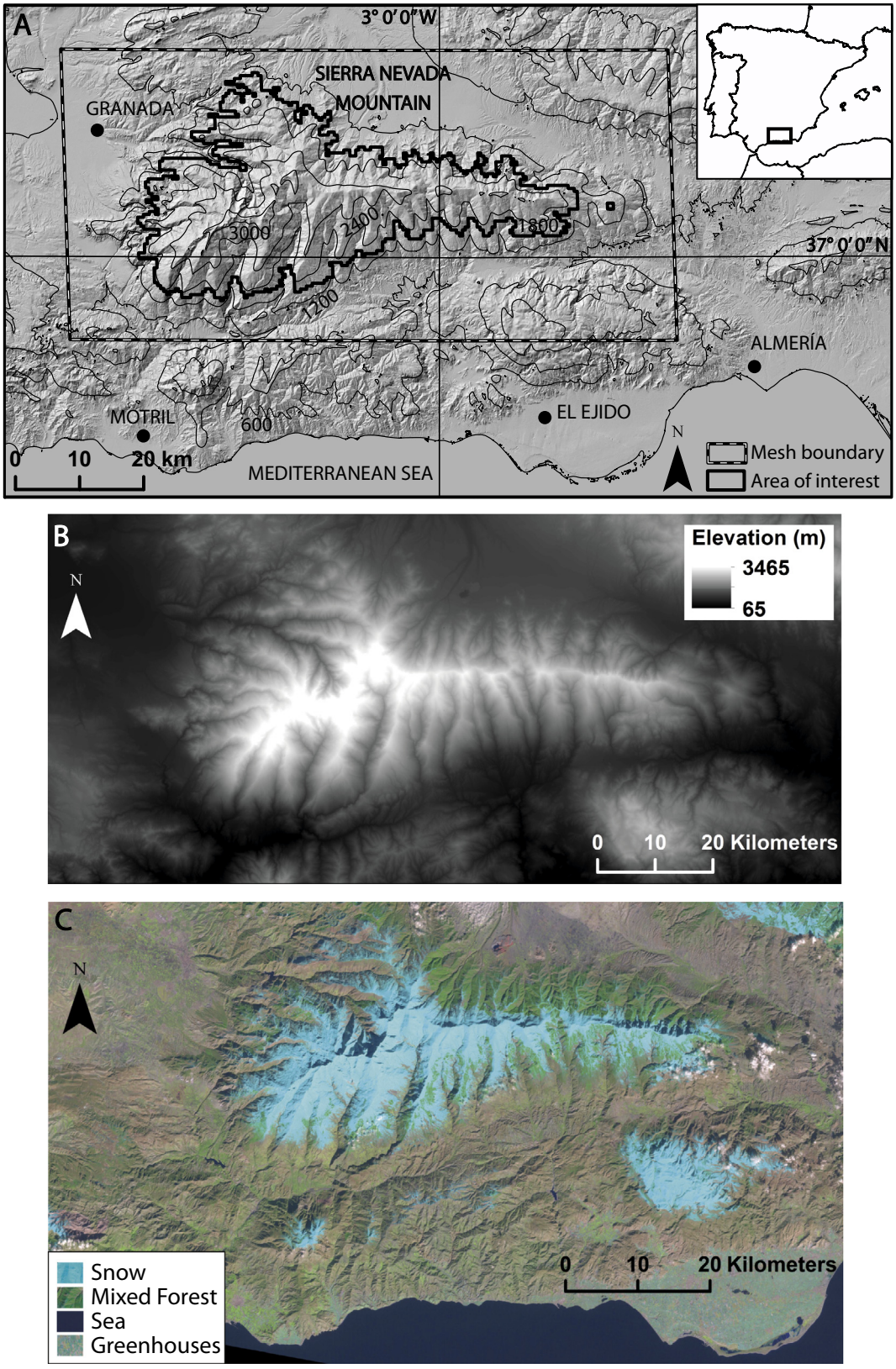

Fig. 1. A: Location of the Sierra Nevada mountain range in Southern Spain. B: the digital elevation model of the study area. C: Landsat image, provided by the USGS, that shows the snow covered area in Sierra Nevada for the date 20/01/2000.

The procedure used to choose the best climatological indices was to obtain a first best estimation of the model parameters P_0, a, b, T_c, N_m and then compare the results with each pair of indices as explained below. These indices are shown with the experimental SCA in Fig. 4. Once the climatological driving variables are chosen, calibration is performed by selecting the optimal

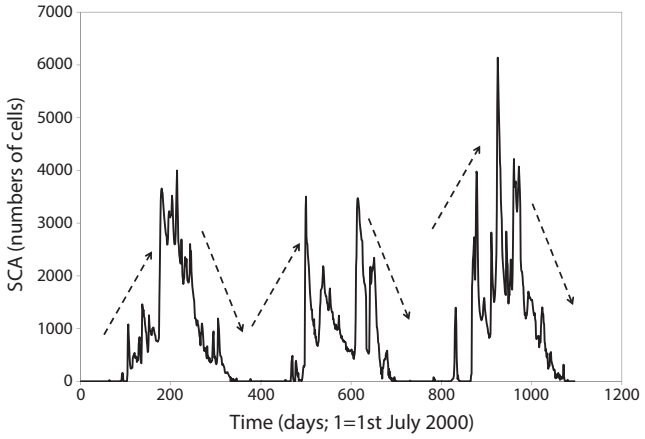

Fig. 2. Daily dynamics of the snow covered area for three consecutive years, from the 1st of July of 2000 to the 30th of June 2003.

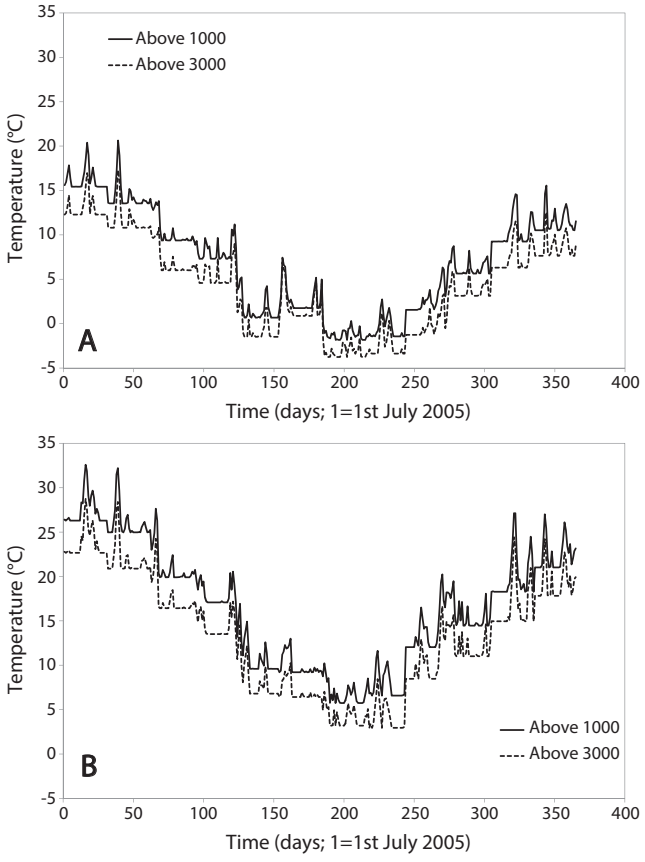

Fig. 3. Daily temperature indexes calculated as A: the mean of the minimum temperatures of the stations of SPAIN02 that are above 1000 and 3000 m and B: the mean of the maximum temperatures of the stations of SPAIN02 that are above 1000 and 3000 m.

values of the parameters P_0, a, b, T_c, N_m that provide unbiased and minimum squared error estimation by comparing the experimental SCA given in Fig. 2, $SCA(t)$, and the estimated SCA from the automata model, $SCA^*(t)$. The estimate is unbiased if the mean error is close to zero and the estimate with minimum squared error is preferred, where the mean error (ME) is defined as:

$$ME = \frac{1}{N}\sum_{t=1}^{N}(SCA^*(t) - SCA(t)) \tag{7}$$

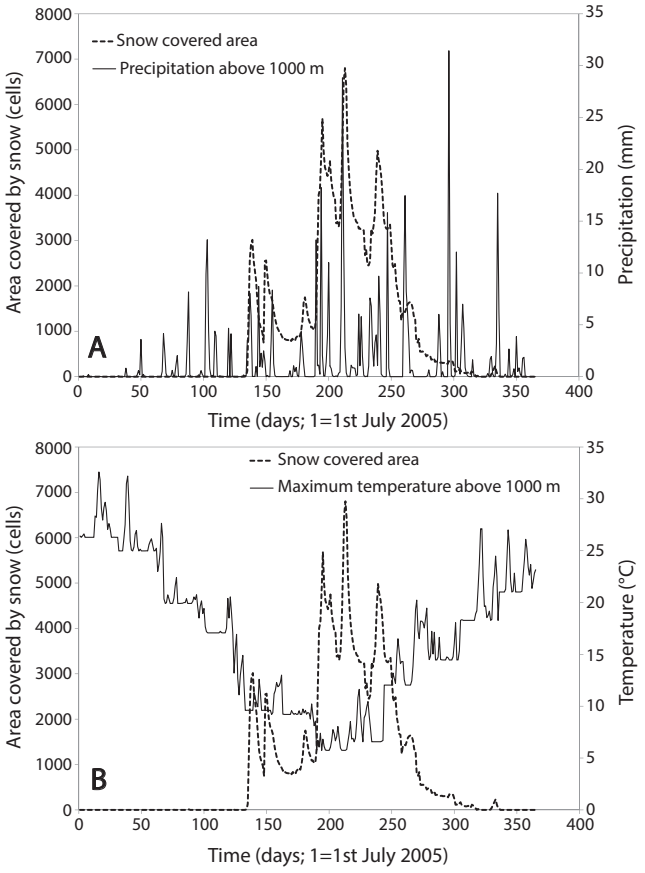

Fig. 4. A: Daily precipitation index (calculated as the mean precipitation from stations of SPAIN02 above 1000 m) and the SCA time series, and B: Daily precipitation index (calculated as the mean maximum temperature from stations from SPAIN02 above 1000 m and SCA) and the SCA time series.

And the mean squared error (MSE) is defined as:

$$MSE = \frac{1}{N}\sum_{t=1}^{N}(SCA^*(t) - SCA(t))^2 \tag{8}$$

Because the number of calibration variables P_0, a, b, T_c, N_m is relatively low (five variables), it is possible to obtain the first estimates by doing an exhaustive search in a coarse grid. Using 10

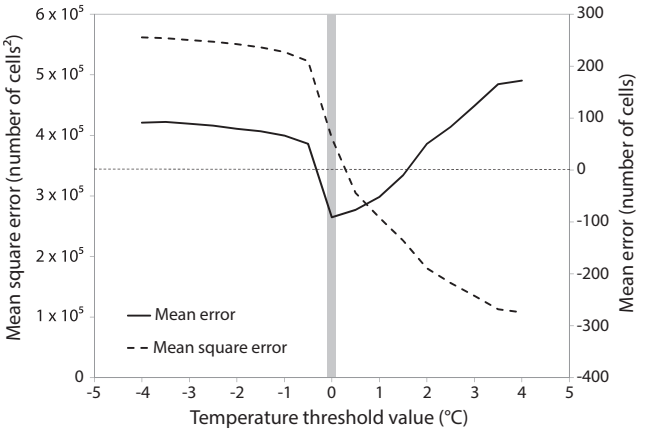

Fig. 5. Mean square error (solid line) and mean error (dashed line) when the only varying parameter is the temperature threshold T_c while the rest of the parameters are hold at their optimal values. It may be seen how the lowest MSE is given by the value of 0 °C which gives also an acceptable ME.

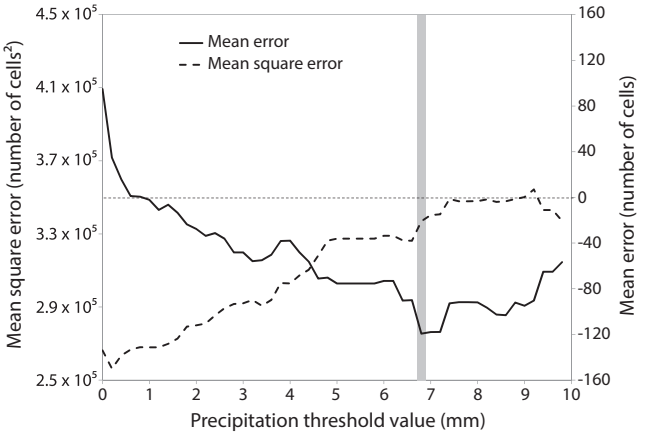

Fig. 6. Mean square error (solid line) and mean error (dashed line) when the only varying parameter is the precipitation threshold while the rest of the parameters are hold at their optimal values. The precipitation threshold with minimum mean square error statistic is 6.8 mm (vertical gray bar) which gives an acceptable mean error of −20 cells.

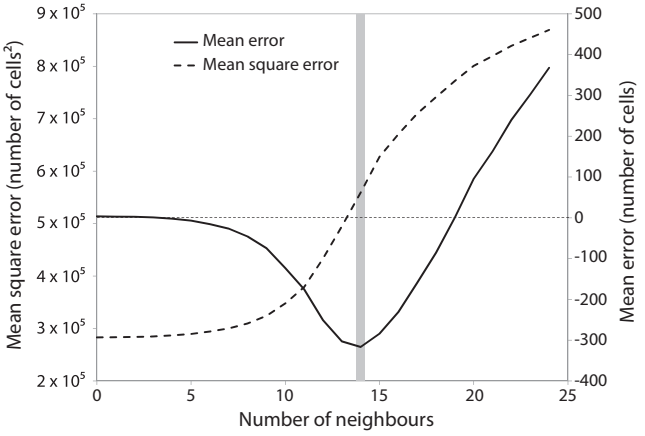

Fig. 7. Mean error (solid line) and mean squared error (dashed line) when the only varying parameter is the number N_m of neighbours with snow which controls if a pixel with snow will change to the state of no snow when temperature increases and there is no precipitation. The N_m with minimum mean square error statistic is 14 (vertical gray bar) which gives an acceptable mean error.

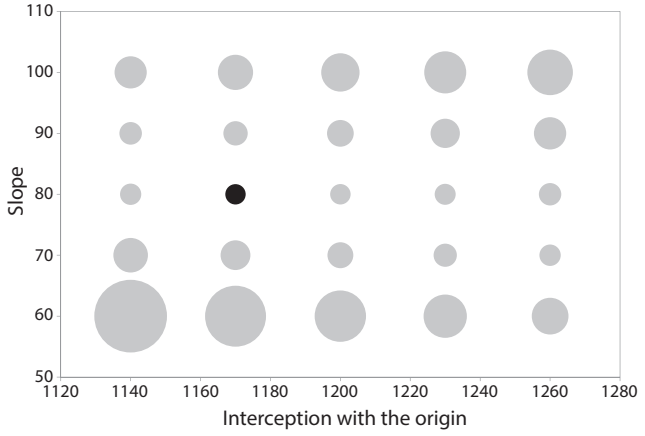

Fig. 8. Mean square error (proportional to the width of the circles) when the only varying parameters are a (interception with the origin) and the parameter b (slope) of the straight line between temperature and altitude of the snow line. The values of 1170 and 80, for a and b respectively, provides the minimum mean square error (solid black circle).

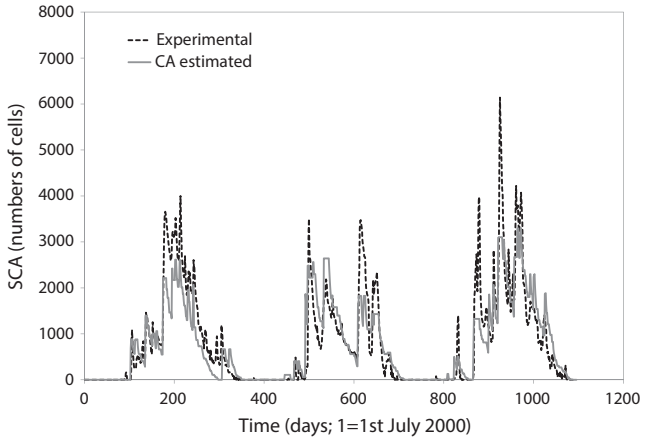

Fig. 9. Experimental SCA and estimated SCA by the calibrated cellular automata model.

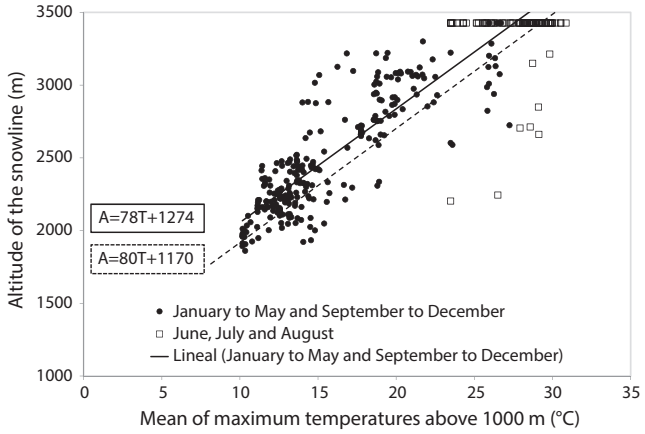

Fig. 10. Experimental lineal relation between temperature and altitude of the snow line for the three years calibration period (dots and solid line) and the independent lineal relation obtained from model calibration (dashed line).

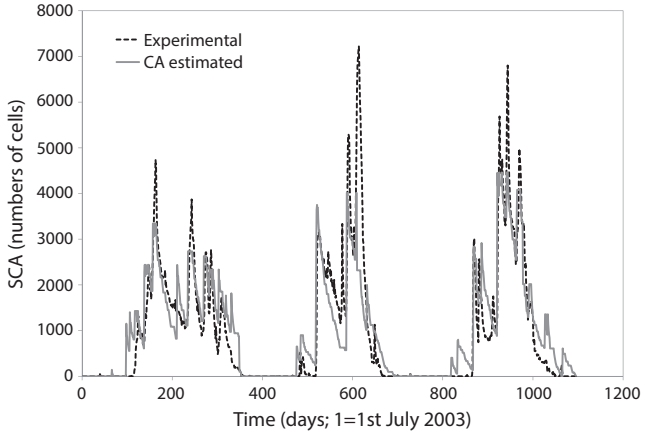

Fig. 11. Experimental SCA and estimated SCA by the calibrated cellular automaton model.

possibilities for each variable there are 10^5 combinations of parameters to evaluate. Next the search is refined by using a finer grid for each parameter while keeping the rest of the parameters fixed at their best estimates. The best estimate for T_c is 0 and the best estimate for N_m is 14 when a neighbourhood of 24 cells (that is a 5×5 neighbourhood) is considered. The best estimate for P_0 is 6.80 mm

while the best estimates for a and b are 1170 and 80 respectively. Fig. 5 shows the ME and MSE as a function of the temperature threshold T_c, while the rest of the parameters are kept to their optimal values. It can be seen how the lowest MSE is given by the value of 0 °C which gives also an acceptable ME. Fig. 6 shows the ME and MSE as a function of the precipitation threshold P_0, while the rest of the parameters are kept to their optimal values. It can be seen how the lowest MSE is given by values of P_0 equal to 6.8 mm which

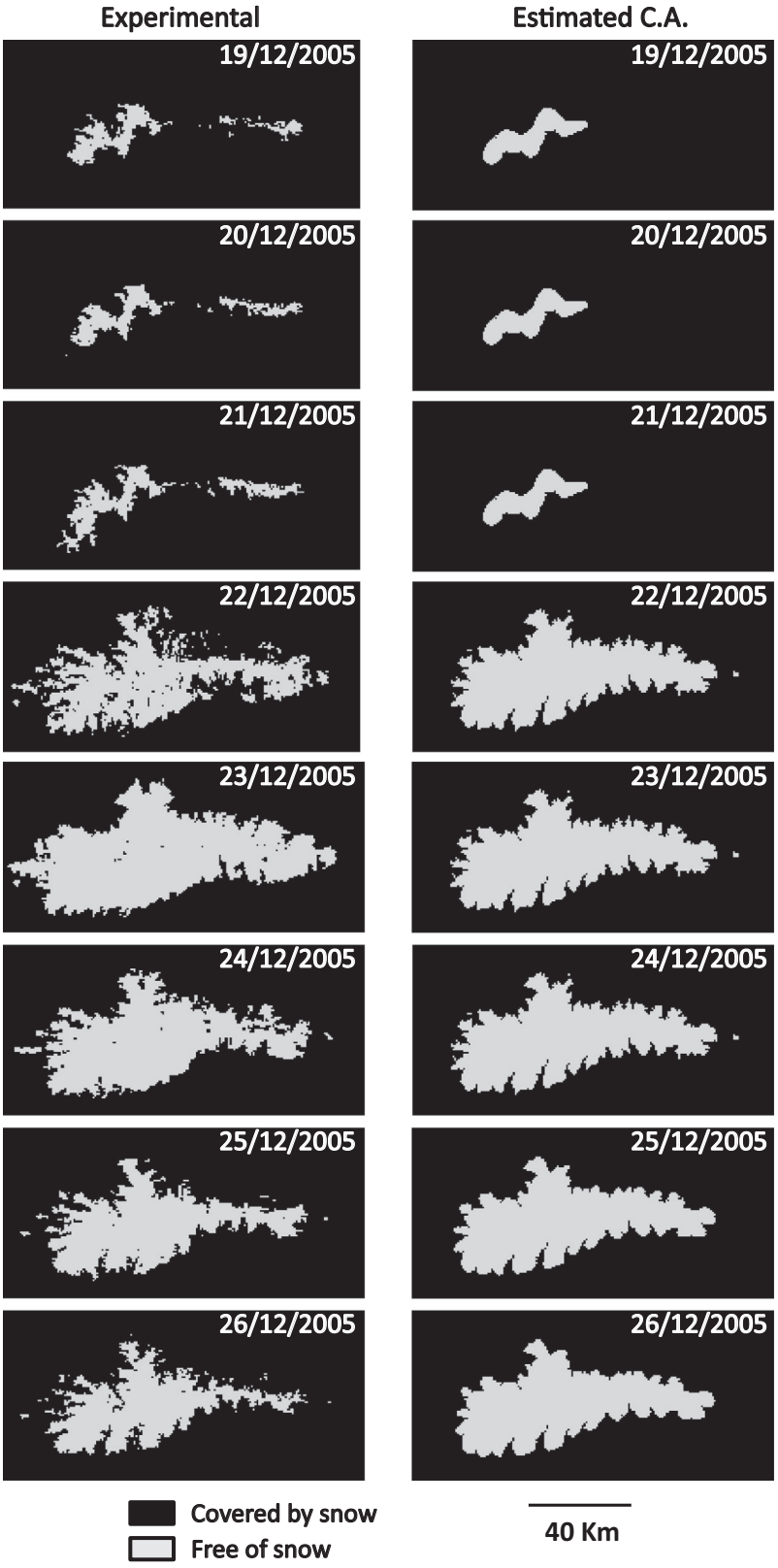

Fig. 12. Spatial daily evolution of the experimental (left) and the estimated by the cellular automaton (right) from the 19th of December 2005 (top) to the 26th of December 2005 (bottom).

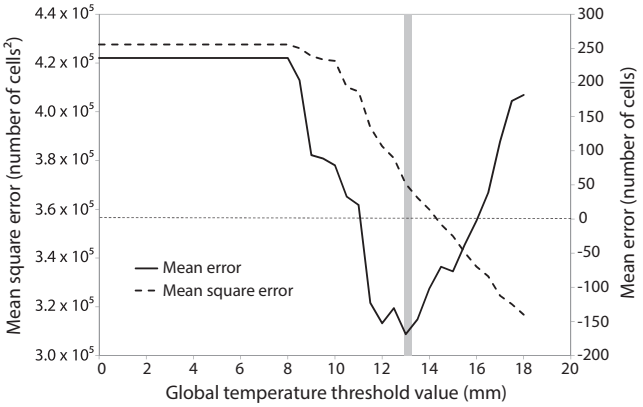

Fig. 13. Mean square error (solid line) and mean error (dashed line) when the only varying parameter is the global temperature threshold T_cc while the rest of the parameters are hold at their optimal values. It may be seen how the lowest MSE is given by the value of 13 °C which gives also an acceptable ME.

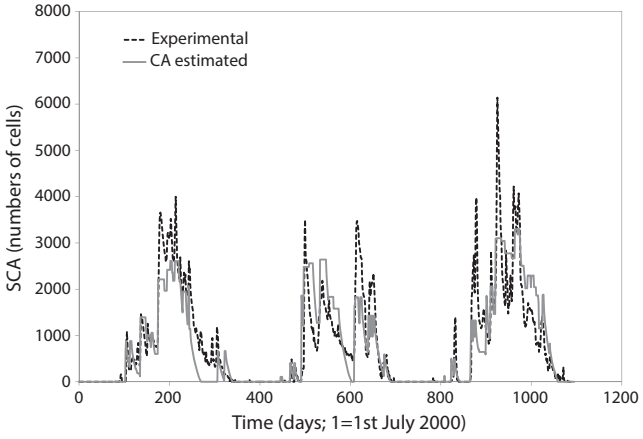

Fig. 14. Experimental SCA and estimated SCA by the calibrated cellular automata model with the global criterion given in Eq. (9).

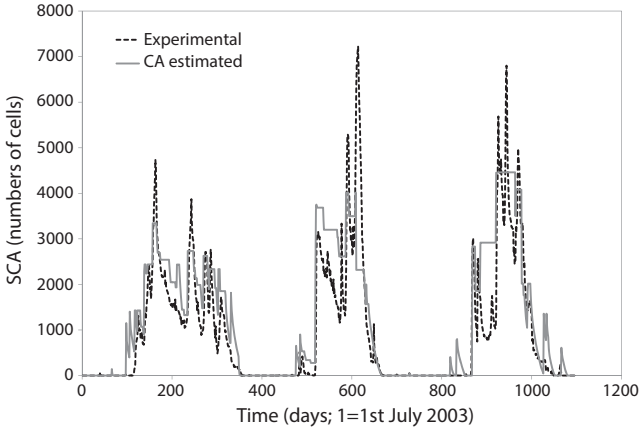

Fig. 15. Experimental SCA and estimated SCA by the calibrated cellular automaton model with the global criterion given in Eq. (9).

also results in an acceptable ME. Fig. 7 shows the ME and MSE as a function N_m when a neighbourhood of 24 cells (that is a 5×5 neighbourhood) is considered. The estimated value is 14, which gives the minimum MSE and a reasonable ME. Fig. 8 shows the ME and MSE as a function of the calibration parameters a and b respectively. Thus the best calibration values for the variables P_0, a, b, T_c, N_m are 6.8, 1170, 80, 0 and 14 respectively.

When the cellular automaton model is applied with these parameters, the estimated dynamics of daily SCA are obtained and have been represented in Fig. 9. The mean error is 62 cells and the mean squared error is 264896. It can be seen from Fig. 9 that the main discrepancy is that the maximum experimental SCA with very fast dynamics is only partially captured. One explanation for this may be that the change in the snowline over time does not follow a straight line for the whole year but two different straight lines, one for the winter months and another for the rest of the year. We have observed this when the data are averaged for a large number of years. However, for the three year period the relationship is not as clear, as may be seen in Fig. 10. Thus, this issue is left open for future research to improve the cellular automaton. Nevertheless, Fig. 10 shows how the linear relationship between snowline altitude and temperature obtained from the experimental data (MODIS binary images, the digital elevation model and the temperature driving variable) is similar to the optimal values obtained by calibration and minimization of the mean square error, which speaks to the robustness of the methodology.

The utility of the calibrated model is that it can be applied in operational mode to another time interval that was not used in the calibration and where there are not experimental SCA data. However in this study where the main task was to present the methodology and its performance, the method has been applied to another time interval not used in calibration, but where the SCA is known so it can be compared to the model's prediction. This process is shown in Fig. 11, which shows the experimental SCA from 1July 2003 to 30 June 2006 and the estimated evolution of the SCA. The ME is -49 cells and the MSE is 451212. Obviously the MSE is worse than in the calibration period but it can be seen how the bulk of the evolution has been captured and could provide useful results for application. Finally, Fig. 12 shows the spatial evolution of the daily SCA for the 8 days from 19 to 26 December 2005, which correspond to the main peak in Fig. 11 around day 177. It can be seen how the main features of the SCA are captured in the values estimated using the cellular automaton model.

The cellular automaton model may be modified in different ways so as to improve its final performance. Some are left for future research but one that should be examined here is the following. The rule described in Eqs. (2) and (3) seems to have less of an explanation than a global rule as follows:

- If precipitation at day t is below the threshold$P(t) < P_0$ and the temperature has decreased or has increased by an amount smaller than a given threshold:

$$T(t) > T_{cc} \tag{9}$$

By calibrating the cellular automaton with this new rule the optimal value of T_{cc} is 13 °C (Fig. 13). Although this rule seems to make more physical sense than the other rule, the results of MSE of 308760 for calibration (Fig. 14) and 580121 for validation (Fig. 15) are clearly worse than the rules in Eqs. (2) and (3).

4. Conclusions

Cellular automata models have been presented to estimate daily snow cover dynamics in the Sierra Nevada mountain range in southern Spain. The area has been discretized with a cell size equal to the size of the MODIS pixel. The snow covered area from the MODIS snow covered area product was used to calibrate the cellular automaton model. Lumped climatological indexes were introduced in order to reproduce realistic dynamics in the study area, given that in summer the snow covered area is null (thus the whole area has a constant value of zero) and therefore a pure cellular automaton would fail. The model must be calibrated using

five parameters: a precipitation threshold, the parameters of a straight line that define the snowline altitude as a function of temperature, and two pure cellular automata parameters. Of the latter, the first parameter is the size of the neighbourhood considered in the dynamics of each cell and it has been set as a 5×5 neighbourhood so the central pixel has 24 neighbours. The second parameter is the number N_m of neighbours with snow, which controls if a pixel with snow will change to the state of no snow when the temperature increases and there is no precipitation. The optimal number N_m was 14. The results obtained with the calibrated model when it is applied in operational mode to a different time period can be judged as satisfactory, as the main events of the dynamics are captured by the calibrated model. The introduction of spatially distributed climatological indices is left open for future research.

Acknowledgements

This research was funded by the research projects CGL2013-48424-C2-2-R and CGL2015-71510-R from the "Ministerio de Economía y Competitividad" of Spain. We would also like to thank the NASA DAAC for the SCA data and the Spain02 project (Herrera et al., 2012) for the climatic data employed in this project. We would like to thank the anonymous reviewers for providing constructive criticism.

References

Alvarado Montero, R., Schwanenberg, D., Krahe, P., Lisniak, D., Sensoy, A., Sorman, A. A., Akkol, B., 2016. Moving horizon estimation for assimilating H-SAF remote sensing data into the HBV hydrological model. Adv. Water Resour. 92, 247–248. http://dx.doi.org/10.1016/j.advwatres.2016.04.011.

Barpi, F., Borri-Brunetto, M., Delli Veneri, L., 2007. Cellular-automata model for dense-snow avalanches. J. Cold Regions Eng. 21 (4), 121–140.

Bormann, K.J., Westra, S., Evans, J.P., McCabe, M.F., 2013. Spatial and temporal variability in seasonal snow density. J. Hydrol. 484, 63–73.

Bruland, O., Maréchal, D., Sand, K., Killingtveit, Å., 2001. Energy and water balance studies of a snow cover during snowmelt period at a high arctic site. Theoret. Appl. Climatol. 70, 53–63.

Collados-Lara, A.J., Pardo-Iguzquiza, E., Pulido-Velazquez, D., 2017. Spatio-temporal estimation of snowpack thickness using point data from snow stakes, digital terrain models and satellite data. Hydrol. Process. http://dx.doi.org/10.1002/hyp.11165.

Elder, K., Rosenthal, W., Davis, R.E., 1998. Estimating the spatial distribution of snow water equivalence in a montane watershed. Hydrol. Process. 12 (10–11), 1793–1808.

Escriva-Bou, A., Pulido-Velazquez, M., Pulido-Velazquez, D., 2017. The economic value of adaptive strategies to global change for water management in Spain's jucar basin. J. Water Resources Plan. Manage. http://dx.doi.org/10.1061/(ASCE)WR.1943-5452.0000735.

Fernandez-Montes, S., Rodrigo, F.S., 2015. Trends in surface air temperatures, precipitation and combined indices in the southeastern Iberian Peninsula (1970–2007). Climate Res. 63 (19), 43–60. http://dx.doi.org/10.3354/cr01287.

Foster, J., Liston, G., Koster, R., Essery, H., Behr, H., Dümenil, L., Verseghy, D., Thompson, S., Pollard, D., Cohen, J., 1996. Snow cover and mass intercomparisons of general circulation models and remotely sensed data. J. Clim. 9, 409–426.

Hall, D.K., G.A. Riggs, V.V. Salomonson, 2006. MODIS/Terra Snow Cover 5-Min L2 Swath 500m. Version 5. Boulder, Colorado USA: NASA National Snow and Ice Data Center Distributed Active Archive Center. http://dx.doi.org/10.5067/ACYTYZB9BEOS.

Hall, D.K., Riggs, G.A., 2007. Accuracy assessment of the MODIS products. Hydrol. Process. 21, 1534–1547.

Herrera, S., Gutiérrez, J.M., Ancell, R., Pons, M.R., Frías, M.D., Fernández, J., 2012. Development and analysis of a 50-year high-resolution daily gridded precipitation dataset over Spain (Spain02). Int. J. Climatol. 32, 74–85.

Herrera, S., Fernández, J., Gutiérrez, J.M., 2016. Update of the Spain02 gridded observational dataset for Euro-CORDEX evaluation: assessing the effect of the interpolation methodology. Int. J. Climatol. 36, 900–908. http://dx.doi.org/10.1002/joc.4391.

Hou, J.L., Huang, C.L., 2014. Improving mountainous snow cover fraction mapping via artificial neural networks combined with MODIS and ancillary topographic data. IEEE Trans. Geosci. Remote Sens. 52 (9), 5601–5611.

Jacob, D., Petersen, J., Eggert, B., Alias, A., Christensen, O.B., Bouwer, L., Braun, A., Colette, A., Déqué, M., Georgievski, G., Georgopoulou, E., Gobiet, A., Menut, L., Nikulin, G., Haensler, A., Hempelmann, N., Jones, C., Keuler, K., Kovats, S., Kröner, N., Kotlarski, S., Kriegsmann, A., Martin, E., Meijgaard, E., Moseley, C., Pfeifer, S., Preuschmann, S., Radermacher, C., Radtke, K., Rechid, D., Rounsevell, M., Samuelsson, P., Somot, S., Soussana, J.-F., Teichmann, C., Valentini, R., Vautard, R., Weber, B., Yiou, P., 2013. EURO-CORDEX: New High-Resolution Climate Change Projections for European Impact Research Regional Environmental Change. Springer, Berlin Heidelberg, pp. 1–16.

Kumar, U., Mukhopadhyay, C., Ramachandra, T.V., 2014. Cellular automata calibration model to capture urban growth. Boletín Geológico y Minero 125 (3), 285–299.

Leguizamón, S., 2006. Simulation of snow-cover dynamics using the cellular automata approach. In: 8th International Symposium on High Mountain Remote Sensing Cartography, 41, pp. 87–92.

Lindström, G., Johansson, B., Persson, M., Gardelin, M., Bergström, S., 1997. Development and test of the distributed HBV-96 hydrological model. J. Hydrol. 201, 272–288.

Lopez-Moreno, J.I., Fassnacht, S.R., Heath, J.T., Jonas, T., 2013. Small scale spatial variability of snow density and depth over complex alpine terrain: Implications for estimating snow water equivalent. Adv. Water Resources 55, 40–52. http://dx.doi.org/10.1016/j.advwatres.2012.08.010.

Martinec, J., Rango, A., Roberts, R., 2008. Snowmelt Runoff Model SRM User's Manual. New Mexico State University, pp. 178.

Mir, R.A., Jain, S.K., Saraf, A.K., Goswami, A., 2015. Accuracy assessment and trend analysis of MODIS-derived data on snow-covered areas in the Sutlej basin, Western Himalayas. Int. J. Remote Sens. 36 (15), 3837–3858.

Mishra, B., Tripathi, N.K., Babel, M.S., 2014. An artificial neural network based snow cover predictive modeling in the higher Himalayas. J. Mt. Sci. 114, 825–837.

Molotch, N.P., Fassnacht, S.R., Bales, R.C., Helfrich, S.R., 2004. Estimating the distribution of snow water equivalent and snow extent beneath cloud cover in the Salt-Verde River basin, Arizona. Hydrol. Process. 18 (9), 1595–1611.

Pulido-Velazquez, D., Garrote, L., Andreu, J., Martin-Carrasco, F.J., Iglesias, A., 2011. A methodology to diagnose the effect of climate change and to identify adaptive strategies to reduce its impacts in conjunctive-use systems at basin scale. J. Hydrol. 405, 110–122. http://dx.doi.org/10.1016/j.jhydrol.2011.05.014.

Pulido-Velázquez, D., García-Aróstegui, J.L., Molina, J.L., Pulido-Velázquez, M., 2015. Assessment of future groundwater recharge in semi-arid regions under climate change scenarios (Serral-Salinas aquifer, SE Spain). Could increased rainfall variability increase the recharge rate? Hydrol. Process. 29 (6), 828–844. http://dx.doi.org/10.1002/hyp.10191.

Quintana-Seguí, P., Turco, M., Herrera, S., Miguez-Macho, G., 2016. Validation of a new SAFRAN-based gridded precipitation product for Spain and comparisons to Spain02 and ERA-Interim. Hydrol. Earth Syst. Sci. Discuss. http://dx.doi.org/10.5194/hess-2016-349.

Reiter, C.A., 2005. A local cellular model for snow crystal growth. Chaos, Solitons Fractals 23, 1111–1119.

Richer, E.E., Kampf, S.K., Fassnacht, S.R., Moore, C.C., 2013. Spatiotemporal index for analyzing controls on snow climatology: application in the Colorado Front Range. Phys. Geogr. 342, 85–107.

Sensoy, A., Uysal, G., 2012. The value of snow depletion forecasting methods towards operational snowmelt runoff estimation using MODIS and numerical weather prediction data. Water Resour. Manage. 2612, 3415–3440.

Sexstone, G.A., Fassnacht, S.R., 2014. What drives basin scale spatial variability of snowpack properties in northern Colorado? Cryosphere 82, 329–344.

Thirel, G., Salamon, P., Burek, P., Kalas, M., 2013. Assimilation of MODIS snow cover area data in a distributed hydrological model using the particle filter. Remote Sens. 5, 5825–5850. 103390/rs5115825.

Wolfram, S., 1984. Cellular automata: a model of complexity. Nature 31, 419–424.